Check for updates

3D printing of tailored veterinary dual-release tablets: a semi-solid extrusion approach for metoclopramide†

Rathna Mathiyalagan,[a] Max Westerlund,[a] Alaa Mahran,[a] Rabia Altunay,[b,c] Jarkko Suuronen,[b] Mirja Palo,[a] Johan O. Nyman,[a] Eero Immonen,[c] Jessica M. Rosenholm, [iD] *[a] Erica Monaco[a] and Xiaoju Wang*[a]

Metoclopramide (MCP) is frequently used to control nausea and vomiting in animals, but its short half-life requires it to be administered thrice daily. In addition, commercial veterinary MCP formulations are currently lacking. As a result, veterinary practitioners often resort to off-label use of human medications, which can lead to inconsistent patient outcomes and complications arising from inadequate dosing. Thus, there is a growing recognized need for individualized treatment strategies also within veterinary practice, as they can offer tailored doses and improved options for animal patients. To address this unmet need and overcome these challenges, our study focused on developing a once-daily dual-release tailored dose for different-sized cats and dogs utilizing semi-solid extrusion (SSE) 3D printing. The dual-release system containing different cellulosic polymers is designed to provide a rapid onset and sustained action to ensure prolonged drug release and minimize the frequency of administration. The produced printing ink formulations were successfully used to obtain different-sized tailored doses with a significant correlation between the designs and the obtained drug amounts. Dissolution studies revealed the impact of polymer combinations and tablet surface area on drug release profiles. Kinetic modeling indicated that both diffusion and erosion are involved in the release mechanisms. This research emphasizes the practical use of SSE 3D printing in developing dual-release delivery systems by producing precise and pet-friendly tailored tablets to enhance veterinary treatments close to the point-of-care.

Introduction

Nausea and vomiting are the most common issues that occur alone or together; they arise from improper diet, underlying medical conditions like gastritis, or treatments such as chemo- and radiotherapy. These symptoms not only affect humans but also cause significant distress in animals.[1–3]

Metoclopramide (MCP) is highly water-soluble due to its hydrochloride salt form. It is a dopamine D2 receptor antagonist recognized for its anti-emetic and prokinetic properties.[4,5] The substituted benzamide ring in MCP allows interaction with receptors in the central nervous system and the gastrointestinal tract, making it practical for managing nausea and vomiting in humans and animals, including cats and dogs.[6,7] MCP has a short biological half-life of 2.5–5 h and typically requires continuous administration to maintain therapeutic levels.[5,8] Currently, no MCP animal products are approved by the European Medical Agency (EMA) or the US Food and Drug Administration (FDA). Therefore, veterinarians often prescribe human formulations off-label for cats and dogs, with a recommended oral dose of 0.2 to 0.5 mg kg^{-1} every 8 h.[5,9–11] To fill this gap, MCP has been compounded from human-use medications, allowing for greater flexibility in treating a range of species and sizes in veterinary practice.[12,13]

A standard treatment approach often involves using one-size-fits-all tablets produced by traditional mass-production methods.[14] However, the one-size-fits-all treatment strategy can lead to different challenges, such as formulation errors, inaccurate dosing, limited customization, difficulties in achieving a steady release, and poor patient compliance.[15–17] The tailored medicine approach would be a great alternative to the one-size-fits-all treatment, as this provides suitable dosing to

[a] Pharmaceutical Sciences Laboratory, Faculty of Science and Engineering, Åbo Akademi University, Tykistökatu 6A, 20520 Turku, Finland. E-mail: jessica.rosenholm@abo.fi, xiaoju.wang@abo.fi

[b] School of Engineering Sciences, Lappeenranta-Lahti University of Technology LUT, Yliopistonkatu 34, 53850 Lappeenranta, Finland

[c] Computational Engineering and Analysis Research Group, Turku University of Applied Sciences, Joukahaisenkatu 3, 20520 Turku, Finland

† Electronic supplementary information (ESI) available. See DOI: https://doi.org/10.1039/d4pm00322e

meet individual patient needs and potentially revolutionizes the current animal healthcare system, allowing veterinarians with many options to achieve improved treatments. Additive manufacturing (AM), or 3D printing technology, has been recognized as a promising technology capable of producing both simple and complex designs in a controlled manner. The inclusion of AM technologies in pharmaceutical fabrication allows for precise dosing and the customization of release profiles by altering tablet structures and geometries.[18,19] Semi-solid extrusion (SSE) 3D printing technique would be the alternative solution to overcome these challenges by providing precise medicine to patients according to their body weight, size, and disease severity. This process involves 3D printing of semi-solid paste and gel-like ink formulations by layer-by-layer extrusion, offering precise control while printing complex designs. The usage of disposable syringes in SSE 3D printing minimizes the risk of contamination compared to the tablet-pressing method.[20–22] This robust technology allows manufacturing at low temperatures, making it suitable for thermo-sensitive excipients and active pharmaceutical ingredients (APIs). SSE 3D printing is highly dependent on the rheological properties of printing ink formulation. Therefore, it is important to evaluate the viscoelastic properties of printing inks before 3D printing. A homogeneous formulation with no phase separations as printing ink is expected to provide uniform distribution throughout the tablet, resulting in precise and flexible dosage forms. These advantages make SSE an appropriate method for manufacturing tailored doses on-demand, close to the point-of-care.[23–26]

In this study, tailored doses of dual-release tablets were compounded by SSE 3D printing to reduce frequent dosing and achieve stable drug release. The prepared formulation is intended to provide quick-onset actions and a slow release over an extended time for different-sized cats and dogs by reducing the frequency of administration. Developing a dual-release matrix system using the same or different APIs offers cost-effective treatment, flexible formulation design, reduces the adverse effects of frequent dosing, and dosing convenience design.[27–29] Furthermore, this delivery system eases the administration difficulties for pet owners and veterinarians, resulting in safe treatments, improved patient compliance, and treatment outcomes.

In the past two decades, many researchers have employed 3D printing technologies to achieve more complex drug-delivery systems to meet the challenges associated with traditional compounding by conventional methods and to achieve stable, personalized drug-delivery systems.[30] Zhang *et al.* developed combi-pills containing model drugs tranexamic acid and indomethacin using SSE 3D printing technology coupled with fused deposition modeling (FDM).[31] A bilayer tablet containing diclofenac sodium sustained-release drug delivery system was produced coupled with hot melt extrusion and FDM.[32] In addition, Genina *et al.* and Ghanizadeh Tabriz *et al.* used FDM to develop a controlled-release bilayer tablet containing a combination of two anti-tuberculosis drugs, rifampicin and isoniazid.[33,34] Two published studies found dual-release

systems developed using SSE 3D printing techniques; namely, Khaled *et al.* manufactured a bi-layer tablet containing guaifenesin as a model drug, and Fang *et al.* prepared an ofloxacin-containing dual-release system.[35,36]

To the extent of our knowledge, no studies have developed tailored doses containing MCP using 3D printing technologies. In this study, we aim to manufacture four different-sized dual-release tailored dose tablets for cats and small to medium-sized dogs utilizing SSE 3D printing. We developed a formulation system with widely used cellulosic polymers to achieve immediate and extended release in one tablet matrix system. We hypothesize that the prolonged release could be achieved by swelling such polymers, forming a gelling layer when in contact with water. Hydroxypropyl methylcellulose (HPMC) was used to prepare the immediate-release (IR) formulation. For the extended-release (ER) formulation, a combination of hydrophilic and hydrophobic polymers was utilized, namely hydroxypropyl cellulose (HPC), sodium carboxymethyl cellulose (CMC), and ethyl cellulose (EC) was used as primary matrix forming materials. Liver powder (LP) was incorporated into the IR formulation to enhance the taste and palatability of the tablets. The developed formulations were successfully used to fabricate tailored doses using SSE 3D printing, which exhibited sufficient mechanical properties. The drug release profile and kinetics were investigated on the fabricated dual-release tablets. Our study findings address the current veterinary treatment landscape and provide improved treatment options for small animals by offering tailored doses that minimize the need for off-label treatments. The obtained dual-release tablets, using advanced technology, provide safe and efficient treatments in veterinary practice.

Materials

Metoclopramide hydrochloride (MCP) was purchased and used as the API (Sigma Aldrich, St Louis, MO, USA). The immediate-release (IR) formulation was first screened with various grades of hydroxypropyl methylcellulose (HPMC) polymer, Methocel K3 Premium, which was kindly donated by Dupont (Luzern, Switzerland). Crospovidone (Kollidon CL), a super disintegrant, was kindly donated by BASF (Ludwigshafen, Germany), and D-mannitol (Ph. Eur., Merck, Darmstadt, Germany) was purchased to use as a filler and a disintegration enhancer in the formulations. Glycerol 85% (Fagron, Barsbüttel, Germany) and pure liver powder (LP) (CC Moore & Co., Stalbridge, UK) were purchased and used as a plasticizer and taste enhancer.

The extended-release (ER) formulation was screened separately with different polymers to formulate a matrix system. Klucel™ XTEND hydroxypropyl cellulose (HPC), HPC JXF Pharm, was kindly gifted by Ashland (Schaffhausen, Switzerland). Microcrystalline cellulose (MCC), Avicel® PH 101™ (Orion, Finland), and Blanose™ sodium carboxymethyl-cellulose (CMC) (Schaffhausen, Switzerland) were kindly donated and used as a filler and release modifier. Ethyl cell-

ulose (EC) was purchased from (Sigma Aldrich St Louis, MO, USA), and used as a release modifier. Polyvinyl alcohol-polyethylene glycol graft copolymer PEG-PVA (Kollicoat® Protect KP) (Ludwigshafen, Germany) was kindly donated and used as a binder to enhance the smoothness of formulations. Ethanol (EtOH), 96% v/v (VWR International, France), and purified water (Milli-Q® Merck Millipore, Molsheim, France) were used as solvents. Sodium dihydrogen phosphate (Honeywell Fluka™, Seelze, Germany), potassium dihydrogen phosphate (Merck, Germany), and 37% hydrochloric acid (HCl) were purchased from Sigma Aldrich (Steinheim, Germany).

Methods

Printing ink formulations

Preparation of ethyl cellulose solution. EC is a hydrophobic cellulosic polymer widely incorporated as a carrier material in matrix tablets, as a binder and thickening agent, and to slow or control the release of drugs.[37] A 12% (w/v) EC solution was prepared by slowly adding the weighed amount of EC to the EtOH to avoid lump forming at 70 °C. The solution was mixed at 500 rpm for 1 h or until dissolved completely. Upon mixing, a translucent colloidal solution was obtained. The solution was then cooled to room temperature and used in the ER formulation.

Preparation of immediate and extended-release paste formulations. The immediate and extended-release paste formulations were prepared individually using the ingredients listed in Table 1. Both formulations were prepared using the traditional mortar and pestle method. MCP is a light-sensitive drug; therefore, formulation preparation was carried out in the absence of light to preserve its stability.

The immediate-release (IR) formulation was prepared by combining all the dry ingredients, including MCP, HPMC, mannitol, and LP. In this formulation, MCP served as API, HPMC polymer acted as a matrix carrier former, mannitol functioned as filler and disintegrant to accelerate the drug

release, and LP was used as a taste enhancer. All these dry compounds were thoroughly mixed until an agglomerate-free mixture was formed. Purified water was added slowly to the powder mixture to avoid lumping and air bubble formation. Due to the addition of LP, a brown-colored homogenously mixed viscous formulation with a suitable consistency for SSE 3D printing was obtained after blending for about 5 minutes.

The extended-release (ER) formulation was prepared in the same manner as the IR formulation. The % of MCP was chosen for each layer concerning the consistency of the paste formulation, ensuring uniform distribution of the drug in the formulation, and the physical size of the final tablet for the facilitation of proper dose administration. HPC was used as a primary matrix former and carrier, CMC and EC as release modifiers, and KP as a binder to refine the consistency of the paste. After mixing all the powders, the 1:1 H$_2$O:EtOH solvent mixture was added slowly to the dry mixture and blended for 5 minutes. A homogenous, white-colored, high-viscosity ER formulation was obtained.

The prepared drug-loaded formulations were carefully transferred to separate 10 mL amber barrel syringes with clear pistons (Nordson EFDLLC, East Providence, RI, USA), and the placebo formulations were transferred to the optimum clear barrel syringes with clear pistons. The prepared formulations were left to rest at room temperature for up to 24 h before 3D printing. The resting time allows the cellulosic polymer network to be fully-fledged, stabilized, and hydrated; this enhances the formulation properties to be suitable for 3D printing. Additionally, it helps maintain consistent formulation while printing, preventing uneven printing results.

Rheology. The rheological properties of the printing ink formulations were analyzed with a HAAKE™ MARS™ 40 Advanced Modular Rheometer system (Version: 4.87.001, Thermo Scientific, Karlsruhe, Germany). The measurements were conducted using HAAKE™ RheoWin job manager software. The viscosity and flow curves of the drug-loaded and placebo formulations were measured using a cone plate geometry with a diameter of 20 mm, 1° cone angle with a default gap of 0.049 mm, and temperature set to 23 °C. Before each measurement, equilibration was achieved with a shear rate of 0 s^{-1} for 60 s.

The flow curve analysis, measuring viscosity $vs.$ shear rate, was carried out on days 0, 1, 14, and 30 in the same manner as in the previous study by Mathiyalagan et $al.$[38] The consistency index was calculated using the power law equation to determine the differences in formulation consistency at different time intervals.[39]

The viscoelastic properties of the ER formulations were investigated through amplitude sweep tests. The tests were carried out by applying a shear strain from 0.0% to 10% at a frequency of 1.6 Hz with 50 data points measured for a duration of 126 s. The relationship between the storage modulus $vs.$ loss modulus (G' $vs.$ G''), the linear viscoelastic region (LVER), was determined to assess the ideal liquid and solid (viscous and elastic) behavior of the printing ink.[40] All the data obtained from different measurements were further analyzed

Table 1 The compositions of different ingredients used in dual-release metoclopramide tablets

Ingredients	Amount in total (% w/w)
Immediate-release layer	
Metoclopramide hydrochloride (MCP)	2
Hydroxypropyl methylcellulose (HPMC K3)	20
Mannitol	35
Liver powder (LP)	1
Purified water (MQ)	42
Total	100
Extended-release layer	
Metoclopramide hydrochloride (MCP)	5
Hydroxypropyl cellulose (HPC)	18
Sodium carboxymethyl cellulose (CMC)	6
Kollicoat protect (KP)	3
12% ethyl cellulose (EC) solution	10
1:1 H$_2$O:EtOH solvent mixture	58
Total	100

with the HAAKE™ RheoWin data manager (Version: 4.87.001, Thermo Scientific, Karlsruhe, Germany). Two measurements were made for each printing ink formulation.

Preparation of dual-release tablet

Optimization of immediate- and extended-release layers. The dual-release tablet containing immediate- and extended-release layers was designed to provide immediate onset with extended therapeutic action effectively. Typically, the IR layer is found to be a smaller portion to achieve quick therapeutic blood levels, and the ER layer has a larger portion with a ratio of 1 : 1, 1 : 2, and 1 : 3, followed by sustained drug release as maintenance dose over an extended time.[21,41] In this study, the drug dosage was chosen as a calculation-based ratio of 1 : 4, *i.e.*, 20% for the IR and 80% for the ER layers to maintain the minimum and maximum effective concentration while also achieving a rapid onset and sustained therapeutic effect.[42] The once-daily tablets of different dose amounts were prepared with targeted doses of 4.5, 7.5, 15, and 22.5 mg for cats and dogs weighing 3, 5, 10, and 15 kg respectively, as shown in Table 2. In this study, 20% of the total drug amount was formulated into the IR and the remaining in ER layers.

Computer-aided designs. Each size tablet was designed using computer-aided design (CAD) software (Autodesk Fusion 360 by Autodesk, San Rafael, CA, USA, 2.0.10446, 2020), a .stl file was imported and sliced prior to 3D printing as presented in Fig. 1. The designs were individually created for each layer, featuring a circular shape with a specific diameter and height to achieve the targeted doses of IR and ER dual-release tablets (Table 2).

Semi-solid extrusion 3D printing

The prepared IR and ER formulations were printed with a 3D BioPrinter (Brinter 1, Brinter Ltd, Turku, Finland) according to the pre-made designs. Two different syringes, one loaded with the IR formulation and the other with the ER formulation, were connected to 20 G and 18 G tapered nozzle tips attached to two different pneumatic tool heads that were heated and cooled, respectively. The 3D designs were imported into the slicing software. The pre-flow was adjusted to 400 and 350 milliseconds for the IR and ER formulations, respectively. Adjusting the pre-flow allows continuous flow by briefly pausing the printhead movement, which helps offset the initial extrusion pressure and ensures smooth material flow. The layer height was set to 0.5 mm, with a shell count of 1, and printed with a grid pattern with an infill density of 1
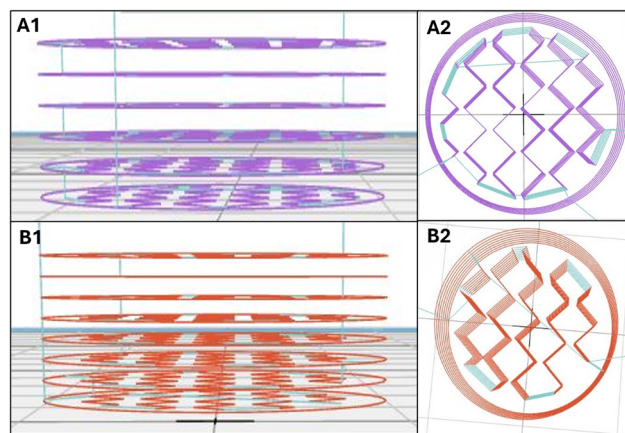

Fig. 1 Computer-aided designs were sliced before 3D printing. (A1) and (B1) show the lateral view of the IR and ER layers. (A2) and (B2) show the top view of each tablet layer.

(100%). The dual-release tablets were produced using an object-by-object printing method at a print speed of 8 mm s^{-1}. The printing pressures were set to 1200 and 3290 mbar for the drug-loaded IR and ER, while their corresponding placebos were printed at 1430 and 3030 mbar, respectively. The IR layer consisted of six, while the ER layer consisted of eight printed layers, with no light exposure during printing. All tablets were printed on transparent poly sheets (Q-Connect A4 copier transparency film, Vow Europe plc, Germany) and were allowed to dry at ambient conditions for 48 h before analysis.

Characterization of dual-release tablets

Physical appearance. The weight of the SSE 3D printed dual-release tablets was evaluated using an analytical balance (Radwag Wagi Elektroniczne, Radom, Poland). The thickness of the tablet was also measured in three areas using a caliper (Absolute Digimatic, Mitutoyo, CD-6″ CX, Kawasaki, Japan). Average and standard deviations were calculated.

Scanning electron microscopy. SEM images were taken using an LEO 1530 Gemini SEM equipped with a Thermo Scientific UltraDry Silicon Drift Detector (SDD, X-ray detector, Oberkochen, Germany). The drug-loaded and placebo dual-release tablets were cut separately with a beam cutter. The material was then coated with platinum before testing with SEM.

Mechanical strength. Mechanical strength must be ensured to validate if the tablets have sufficient durability to withstand post-manufacturing processes such as packaging, transporting, and handleability during administration.

This study conducted hardness and friability tests to examine the 3D printed dual-release tablets. Hardness or crushing strength was tested by measuring the required force (*N*) to break a tablet by compression, which was determined using the Copley Scientific hardness tester (Type TH3, Nottingham, UK). The measurement was conducted on the dual-release tablet; both drug-loaded and placebo tablet dose size 15; the average and standard deviations were calculated

Table 2 The dose amount and the design for immediate and extended-release layers diameter (D) and height (H) of a dual-release tablet to achieve the targeted doses

Targeted doses	4.5 mg	7.5 mg	15 mg	22.5 mg
Dose of IR + ER (mg)	0.9 + 3.6	1.5 + 6	3 + 12	4.5 + 18
IR layer (D × H, mm)	5 × 3.5	6.8 × 3.5	9.5 × 3.5	11.6 × 3.5
ER layer (D × H, mm)	5.5 × 4.5	6.8 × 4.5	9.5 × 4.5	11.6 × 4.5

(n = 6). The relative humidity (RH%) and temperature (°C) were recorded during the measurement. Environmental conditions such as humidity and temperature can significantly affect the tablet's stability.[27] Therefore, moisture content was tested (n = 5) on the drug-loaded tablets, followed by a hardness test, according to Mathiyalagan *et al.*[38]

Performing the hardness test alone is insufficient to evaluate the tablet's quality during handling and packaging. Hence, a friability test was conducted to assess the printed tablets' resistance to mechanical agitation, which may result in weight reduction. The friability test was performed according to European Pharmacopeia (Ph. Eur.),[43] using the friability drummer (Erweka Apparatus GMBH, Heusenstamm, Germany). Tablets with a total weight of 6.5 g were placed inside the drummer and set to run for 100 rotations for 4 minutes. Following this, the tablets were dusted and reweighed to assess the mass loss; typically, a mass loss of less than 1% is deemed acceptable for most pharmaceutical products. Also, to ensure the physical integrity of the uncoated tablets, each tablet was thoroughly examined for any signs of chipping, capping, or tearing due to mechanical stress.[35,44]

Drug content. Drug content analysis is imperative to ensure precise drug content and consistency of drug amount in the 3D printed tailored doses. The drug content was determined by selecting five random dual-release tablets, accurately weighed, and placed in a 250 mL borosilicate amber glass bottle containing 100 mL of purified water as a dissolving medium. The bottles containing tablets were sonicated for 30 min and then placed on the orbital shaker (Multi-Shaker PSU 20 by BIOSAN, Riga, Latvia) at 230 rpm for 12 h. After ensuring the complete dissolving, the samples were diluted (10-fold) and measured at 270 nm with a UV-6300PC double-beam spectrophotometer (VWR International BVBA, Leuven, Belgium); placebo as a reference to exclude possible interferences from the excipients. The data was further analyzed using UV-Vis Analyst software v. 5.44 (VWR International BVBA, Leuven, Belgium). Average and standard deviations (n = 5) were calculated using the equation observed from the calibration curve equation.

Dissolution release profiles

***In vitro* dissolution.** *In vitro* drug dissolution studies were conducted using a basket-type apparatus (Sotax AT 7 Smart, Basel, Switzerland) set to 50 rpm, and the dissolution bath temperature was set to 37 ± 0.5 °C. A series of four dissolution studies were carried out. A different series of dissolution studies was conducted to evaluate the matrix tablet-releasing behavior. Series 1 contained IR drug-loaded and ER placebo tablets; series 2 contained IR placebo and ER drug-loaded tablets; series 3 and 4 contained drug-loaded IR and ER tablets. Series 1–3 were performed mimicking simulated physiological conditions, and series 4 was performed in purified water as a medium. After measuring the weight and thickness of each tablet, the tablets were placed in the vessels containing 500 mL of pH 1.2 (0.1 N HCl) acidic medium for 0–2 h. Later, the medium was replaced with 500 mL of pH 6.8 phosphate

buffer medium, and the study continued for the next 2–24 h. Samples were manually withdrawn at pre-determined time points, diluted with medium, and analyzed by UV-visible spectrophotometer (Lambda 35, PerkinElmer, Singapore) at a wavelength of 271 nm for pH 1.2 and 270 nm for pH 6.8 and purified water, respectively. In addition, a dissolution study was conducted to investigate the release profile of the four different-sized ER doses 4.5, 7.5, 15, and 22.5 to investigate the influences of different surface areas in a pH 6.8 buffer medium. All the measurements were carried out in triplicate, and average and standard deviations were plotted as time against cumulative drug release.

Drug release kinetics. Drug-release kinetics analysis was performed on the obtained dissolution data using the SUBPLEX method and NLopt library interface software applications. The obtained dissolution data were fitted with six different kinetic models. Zero-order and first-order determine the controlled drug release, and the drug release rate decreases rapidly over time. Higuchi's model determines that the drug release of a matrix follows Ficks law-based diffusion behavior, and Hixon Crowell's model shows the drug release that occurred by the changes in the surface area or diameter of the matrix tablet system. The Korsmeyer-Peppas model indicates the Fickian and non-Fickian release behavior, which reveals that one or more combination mechanisms mainly control the drug release. Weibull model is used to compare different matrix formulations of drug release profiles to determine the release profile that does not follow any other models.[45–47]

Stability study

A two-month stability study was conducted on the printed dual-release tablets to investigate their stability upon storage. Size 15 tablets were placed in a petri dish covered with aluminum foil and stored at ambient conditions. Drug content and attenuated total reflectance-Fourier transform infrared spectroscopy (ATR-FTIR) (UATR-2 Spectrum Two, PerkinElmer, Llantrisant, UK) analysis were carried out to analyze the physiochemical properties after 1 and 2 months of storage. The drug content was measured in the same manner as mentioned in the drug content section. ATR-FTIR measurements were carried out according to the previous study by Sjöholm *et al.* to ensure the presence of drugs in the tablet, using pure MCP for comparison.[48]

Results and discussion

Evaluation of printing ink formulations

Evaluating the quality of printing ink formulation is crucial for 3D printing. The materials selection and form of printing ink base have to be evaluated carefully. The developed printing ink must be homogenously mixed, and the drug should be uniformly distributed in the formulation to ensure the fabrication of consistent dosing. Importantly, a printing formulation must exhibit a rheological shear-thinning response to flow consistently through the printing needle and possess strong visco-

elastic properties to recover to its semi-solid status through polymer relaxation after being extruded. The printing ink system also shall warrant the adhesion between the adjacent layers to deliver the printing outcome in shape fidelity.

Generally, desired formulations should be homogeneous in consistency with the drug uniformly dispersed to achieve accurate dosage forms. To be printed with SSE 3D printing technology, the formulation should exhibit shear-thinning and shape retention behavior to maintain the structure during and after printing. Therefore, a paste-like formulation strategy is a convenient way of preparing a formulation suitable for manufacturing using SSE 3D printing technology to obtain a tablet that contains two layers. The formulation's semi-solid behavior aids good adhesion between two layers and supports building layers. In addition, it provides good stability by preventing sedimentation or phase separation issues during printing and upon storage.[49]

Various polymers were initially tested to find suitable polymers and concentrations to prepare a drug delivery system with an IR and an ER layer to achieve dual-drug release. Three formulations were optimized for the IR layer. The first one contained HPMC K3, crospovidone, and glycerol; the second one contained HPMC K3, mannitol, and glycerol. Both formulations were prepared in a one-pot mixing by dispersing the ingredients in water. After stirring overnight, the obtained formulation was foamy, textured, gel-like consistency with small air bubbles. The formulation was manually extruded to investigate the building ability. Due to the film-forming properties of HPMC, the formulation could not keep its shape after extrusion. For 3D printing, the printing inks should be bubble-free to achieve smooth printing and enable accurate dosage forms. After drying at room temperature, the dissolution profile of the extruded tablets did not meet the dissolution acceptance criteria, and the formulations were discarded. The third one contained HPMC K3, mannitol, and LP mixed with water. A paste formulation obtained upon blending showed excellent building ability, kept its shape during and after printing, and was chosen to move forward.

For the ER layer, four different formulations were optimized. The first one contained HPC, MCC, and EC. The second one contained HPC and MCC, and the third one contained HPC, CMC, and EC. All three formulations were mixed with a $1:1$ $H_2O:EtOH$ solvent mixture. All formulations were prepared by mixing with a mortar and pestle; each yielded a thick and gel-like consistency that required a bit more refinement and exhibited poor printability. When performing drug release studies, burst release was observed for most of the formulations. This was probably due to the higher water solubility of MCP and the insufficient polymer concentration in the formulation. These formulations were inadequate as the ER layer aims to achieve steady-state drug release. The fourth formulation consisted of HPC, CMC, EC, and KP blended with $1:1$ $H_2O:EtOH$ solvent. The paste formulation yielded a fine-textured paste formulation with good printability and an extended duration of release profile. Thus, it was chosen as the final formulation for the ER layer.

The final ingredients for the IR formulation are presented in the Table 1. HPMC served primarily as a matrix carrier, providing binding, thickening and gelling properties contributing to a smooth consistency. A higher amount of mannitol also served as a bulking agent, ensuring a formulation free from lumps and bubbles. A brown hue characterized by a strong meat odor due to the addition of LP mixed and blended with water. This homogeneously blended formulation exhibited flowable consistency, enabling the formation of multiple layers, and demonstrated shape retention before and after 3D printing, confirming its suitability for printing.

The final ER formulation was prepared using various ingredients outlined in the accompanying table as IR. The combination of HPC, CMC, and hydrophobic EC polymers developed a finely textured, viscous formulation. This is due to their film-forming, thickening, and binding properties. Additionally, the inclusion of KP enhances moisture protection, improving the paste formulation's overall cohesive behavior. When blended with a $1:1$ $H_2O:EtOH$, we achieved a homogeneous, finely textured, white-colored viscous formulation without bubbles. This resulted in good printability and maintained shape integrity before and after 3D printing.

Rheology

In this study, viscosity and flow curve measurements on the drug-loaded IR and ER and their placebo formulations and viscoelastic properties on the ER drug-loaded and placebo formulations were tested. Assessing the rheological properties of paste-like semi-solid formulations is essential before 3D printing.[40,50] The printing inks should have suitable rheological properties, such as shear-thinning and strong viscoelastic behavior, which show their ability to flow out of the nozzle without clogging at the lower shear rate. Quick recovery after extrusion is essential to achieving and maintaining good printability and shape fidelity.

Viscosity and flow curve. The printability of printing inks is determined by flow curve measurement, which measures their ability to flow under the applied shear rate. The viscosity decreases with increased shear rate, which shows fluids' shear-thinning behavior. Fig. 2 shows the flow behavior of the IR (a) and ER (b) formulations. In the IR formulation, the placebo showed a higher viscosity than the drug-loaded formulation, which can be due to the interaction between the polymer and the drug. HPMC swells by absorbing water, and the presence of MCP in the drug-loaded formulation tends to form hydrogen-bonding interactions with polymers, which interferes with the swelling of polymers by reducing chain mobility. This interaction affects the gel network of HPMC in the matrix and lowers the viscosity. On the other hand, without a drug in the placebo formulation, polymer swelling occurs without any interference, leading to higher viscosity. Such differences in viscosity also resulted in lower pressure when printing drug-loaded compared to the placebo of IR formulation.[51,52]

Contrary to the IR formulation, the drug-loaded ER formulation showed higher viscosity than the placebo formulation, which can be related to the concentration of the drug amount
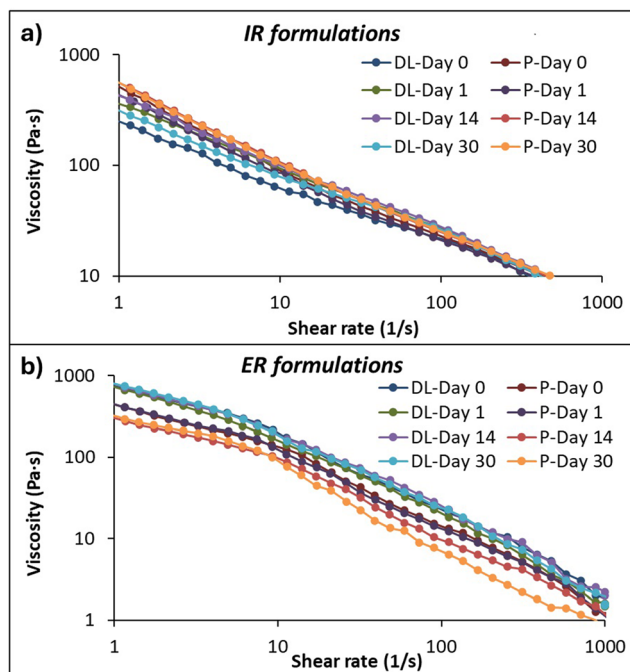
Fig. 2 Rheological measurements of viscosity and flow curves of drug-loaded (DL) and placebo (P) (a) immediate (IR) and (b) extended-release (ER) formulations at days 0, 1, 14, and 30.
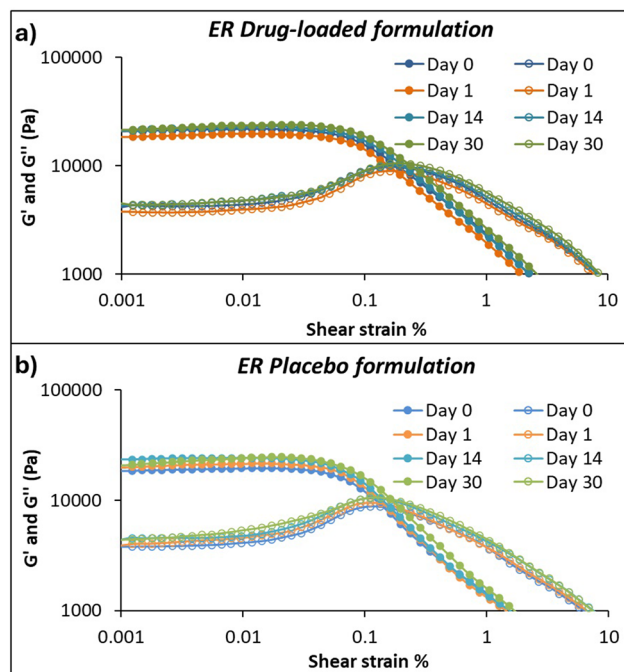

Fig. 3 Rheological measurements of the amplitude sweep test of the extended-release (ER) drug-loaded (a) and placebo (b) formulations on days 0, 1, 14, and 30.

and the polymer concentrations and their properties. Here, the hydrogen bond formation between the drug and more than one polymer causes different interactions, resulting in different swelling behaviors. Also, the hydrophobic interaction of EC with the drug can form strong rigidity, and the anionic nature of CMC interacts with the cationic amine group present in the MCP, resulting in increased viscosity of the formulation.[53,54]

The study was conducted at different time intervals, days 0, 1, 14, and 30, to evaluate the stability and changes in their consistency over time on the IR and ER formulations. Fig. S1† shows the consistency index calculated using power law equations. The viscosity changes due to drug-to-polymer interaction and hydration dynamics over time. No significant differences are seen in the consistency of IR and ER drug-loaded formulations at different time intervals, indicating that the formulation is stable over time. However, the ER placebo formulation had less viscosity on days 14 and 30, possibly due to the polymer relaxation and changes in the entanglement.

Viscoelastic properties. The amplitude sweep test was performed to determine the viscoelastic behavior of the ER drug-loaded and placebo formulations as visualized in Fig. 3. As predicted from the viscosity measurements, the drug-loaded formulation showed higher LVER, which indicates more stable viscoelastic properties than the placebo formulation. This is due to the drug-to-polymer interaction through hydrogen and ions providing more stability by strengthening the matrix system and increasing its resistance to strain.[55] Fig. S2† shows the LVER at different time points. On days 14 and 30, a slight

decrease in the LVER of the placebo formulations was noted. The lower viscosity observed from the viscosity measurements confirmed changes in the formulation, indicating a decrease in viscoelastic behavior over time.

Evaluation of 3D printed tablets

Physical appearance. Two-layer tablets of different sizes containing dual-release profiles were successfully manufactured using SSE 3D printing technology. The average printing time for printing alone the IR layer is 1 min and the ER layer 2 min, and it takes 4 min to print one dual-release tablet. This printing time enhances the feasibility of printing smaller to larger scale production. Furthermore, this supports and is suitable for the on-demand and tailored applications. The 3D printed tablets contained 4.5, 7.5, 15, and 22.5 mg therapeutic doses. Fig. 4 shows a combination of brown and white dual-release tablets with escalating different sizes obtained by SSE 3D printing photographed before and after drying. Microscopic
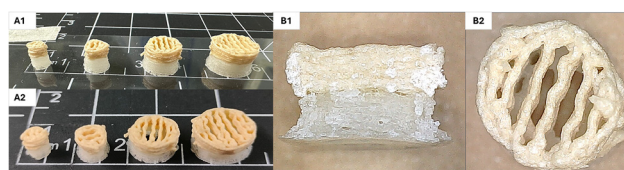

Fig. 4 Photographs showing different-sized dual-release tailored doses before (A1) and after (A2) drying. The microscopic images of the cross-section (B1) and top view (B2) of the dual-release tablets.

images of dual-release tablets' cross-section and surface area (top view) are also shown. The dry and wet weights of the dual-release tablets ranged from 57 to 262 mg and 113 to 525 mg, correlating to the obtained drug amount with R^2 values of 0.9904 and 0.9947, respectively. The IR layer was soft and breakable by hand with a reasonable amount of force. On the contrary, the ER layer was hard, not breakable, and exhibited elastic behavior. Furthermore, ER formulation is tightly compacted by cellulosic polymers, which form a strong network in a matrix system with less porosity. This shows the differences in the formulation design. The microscopic images show that the two layers of the 3D printed tablets adhere well to each other and are not separated during printing and after drying, confirming the polymer-to-polymer interactions in the conjugation layer, interfacing the IR and ER formulation. HPMC and HPC are cellulose polymers with similar structures; they are likely to form hydrogen bonds and entangle with each other, improving the interlayer adhesion.

To summarize, the developed dual-release formulation was intended to support veterinary patients, especially targeting small animals such as cats and dogs. Combining immediate and extended drug release in one tablet addresses the dosing compliance challenges in veterinary medicine. The frequent dosing administration causes distress in pet animals and their owners. SSE 3D printing technology further enables precise and flexible customization dosing, ensuring safe and optimal therapeutic options in veterinary applications. Therefore, beyond improving patient compliance and convenience, this study emphasizes future advancements in tailored veterinary medicines.

Scanning electron microscopy. The surface morphology of IR, lateral view of ER, and cross-cuts of each layer of the dual-release drug-loaded tablet were captured by scanning electron microscope (SEM), as shown in Fig. 5 and the placebo tablets shown in Fig. S4.† Similar morphology was observed on both the drug-loaded and placebo tablets. A rough texture with

more crystals was observed in the IR layer due to the addition of higher concentrations of mannitol in the formulation. Whereas a compacted, smooth texture with less porosity was observed in the ER formulations due to cellulosic polymers. In Fig. S3,† a panorama image shows that the IR and ER layers were achieved with good adherence between each layer, without separation.

Mechanical strength. Hardness and friability are considered essential quality assurance tests in pharmaceutics. They ensure that the prepared tablets comply with the acceptance criteria, assuring product reliability and quality, thus ensuring patient safety.

A too-soft tablet may not withstand handling prior to administration; on the contrary, a too-hard tablet might not disintegrate after administration.[44] To ensure the mechanical strength of the immediate-release layer ($n = 5$), found to be 24.4 ± 0.2 and 12.0 ± 0.6 N, respectively, in the drug-loaded and placebo tablets. That is 2.49 and 1.2 kg, close to the suggested range of 3–7 kg range, considered satisfactory.[56,57] However, the placebo tablet falls under the recommended range. I.e., the addition of drugs makes the tablet harder than placebo tablets, which are likely to have sufficient mechanical strength. Furthermore, this might be due to the porous structure of IR due to the chosen infill pattern and density. Hardness measurements were performed on dual-release tablets ($n = 6$); during the measurement, it was observed that the immediate-release layer was crushed first, and the force was continued to apply until the fracture was noticed in the extended-release layer. The required hardness of a tablet with a minimum of 4 kg is considered to be satisfactory.[44,56] The measured hardness of the drug-loaded and placebo tablets was 39.3 ± 2.3 and 21.8 ± 3.7 N, respectively, which is close to the satisfactory acceptance range. The tests were conducted at ambient conditions with relative humidity and temperature of 60.4 ± 0.5 RH% and 23.2 ± 0.0 °C for drug-loaded tablets and 60.3 ± 0.2 RH% and 22.9 ± 0.1 °C for placebo tablets. The higher strength of the drug-loaded tablets is due to the addition of API, which affects the tablet's properties, leading to differences in the strength and enhancing a longer dissolution profile. The friability test was performed by placing pre-weighed tablets inside the friability drum. The mass loss was found to be within the recommended limit of less than 1%.[5] In combination with the hardness test, the moisture content was recorded since a high level of moisture in the tablet can significantly affect its physio-chemical stability.[58] The moisture content in the dual-release drug-loaded tablets was 2.9 ± 0.5%. The results from the hardness test and friability suggest the printed tablets have sufficient mechanical strength, and the results were found to be within the acceptable range to withstand the handling of the post-manufacturing process.

Drug content. This study aimed to provide accurate, tailored dosage forms; hence, drug content and uniformity were determined in 5 tablets of four different doses, namely, 4.5, 7.5, 15, and 20 mg. The obtained average drug amounts were 5.3 ± 0.20, 8.3 ± 0.30, 17.0 ± 0.81, and 24.9 ± 1.04 mg, respectively,
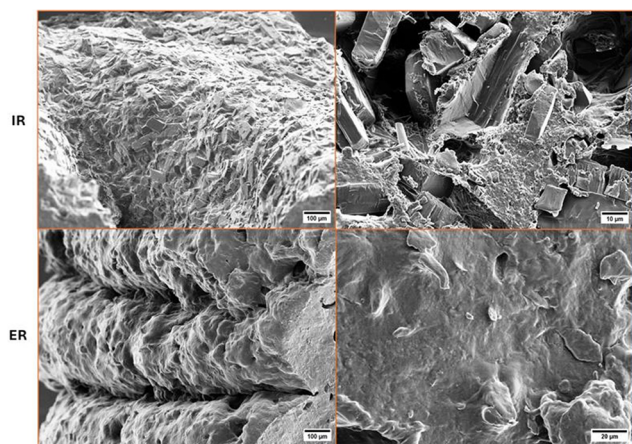

Fig. 5 The left side shows SEM images of the dual-release drug-loaded tablet surface area of immediate (IR) and a lateral view of extended-release (ER), and the right side shows cross-cuts of both layers.

showing a slightly higher drug amount compared to the targeted doses. The printing pressure could be slightly reduced to get an accurate dose amount. A high correlation of $R^2 = 0.9993$ was observed between the area (mm^2) and the drug amount, indicating the ability of SSE 3D printing to produce accurate tailored doses. This ensures that the 3D printing technology efficiently produces tailored dosage forms.

Dissolution release profiles

In vitro **dissolution**. The dissolution release profiles of MCP containing dual-release tablets of four different series were determined. The dry polymer amount in the formulations ranged between 6 and 20%. Increasing polymer concentration increases the formulation viscosity and gelling behavior with a longer diffusion path. This may reduce the drug's effective diffusion coefficient by lowering the drug release rate.[59,60] The gelling behavior of hydrophilic polymers delays the release by swelling when they are in contact with the aqueous medium. This is due to the charged groups of the polymers, which attract water molecules and potentially slow the drug release of a matrix tablet.[61] In contrast, the hydrophobic polymers repel water molecules by forming a hydrophobic matrix in the tablet and preventing water penetration, thus resulting in slow drug release.[37]

The infill density or pore size of the tablet influences the release rate of the drug; 30–50% of the infill rate is mostly considered to obtain a rapid release.[23,34] In our study, the IR layer was printed in a grid pattern with a 100% infill density. Therefore, to confirm the release behavior of an IR formulation, a tablet consisting of only the IR layer was investigated first in a pH 1.2 medium. As expected, rapid drug release was achieved from the immediate release layer; more than 95% of the drug was released within 30 min, as seen in Fig. S5.† In the IR formulation, 20% HPMC was used as the primary matrix carrier; as mentioned, increased polymer concentration forms a strong gelling layer, potentially slowing the drug release. In this case, the amount of HPMC used in the formulation is not high enough to create a viscous gel layer. Also, mannitol, which acts as a disintegrant and pore-forming agent, increases the porosity in the hydrophilic matrix, allowing faster penetration of the dissolution media, thus accelerating the drug release.

Four different series of dissolution studies were performed. Since monitoring the drug release from each layer is difficult with this apparatus setup, the idea was to understand how these two layers act together in the dissolution medium. Therefore, to understand each layer release profile individually, series 1 and 2 were performed. In which, series 1, the IR layer was drug-loaded, and the ER layer was drug-free. In series 2, the IR layer was drug-free, and the ER layer was drug-loaded, as shown in Fig. S6.† The series 1 formulation showed a similar rapid drug release profile to the IR layer alone (Fig. S5†), which confirms that the polymers present in the ER layer formulation do not affect the release of the IR layer. In series 2, 100% drug release was observed within 10 h. Series 3 and 4 dissolution profiles are plotted in Fig. 6a. Series 3 shows the release profile of formulations containing drug-loaded IR
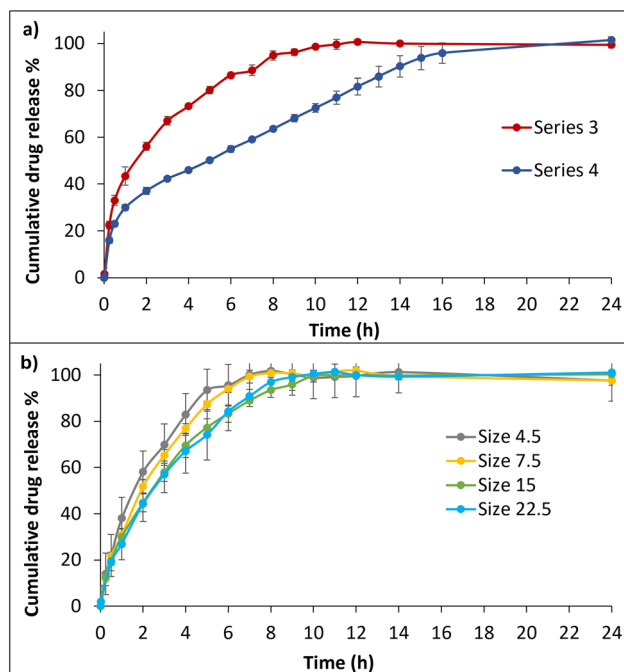

Fig. 6 Drug dissolution release profiles: (a) the 3D printed dual-release tablets in a buffer system (Series 3) and in water (Series 4), and (b) the ER drug-loaded formulation of different-sized tablets in pH 6.8.

and ER layers. At 2 h, 56% drug release was observed in a pH 1.2 medium. In pH 6.8, 98% drug release was achieved within 10 h, and the total drug was released within 12 h. Series 4 shows the release study carried out in the water as a medium to understand the release profile in a neutral medium. A stable and more sustained release profile was achieved by releasing 95% of the drug within 16 h. The studies continued up to 24 h until a stable plateau was reached.

To understand the MCP behavior in different pHs, the acidic conditions were mimicked to simulate the stomach environment where the drug was usually exposed and pH 6.8 buffer mimics the small intestine, where the drug is absorbed after administration of the tablet. In the pH 1.2 acidic environment, MCP is very soluble, but the combination of different polymers controls the release rate, and their properties influence the drug release profile through diffusion and erosion mechanisms, slowing the release rate. HPC and EC are not affected by acidic pH as they are non-ionic polymers but prevent water penetration into the tablet matrix by forming a protective layer. In contrast, the CMC polymer becomes less ionized in the acidic condition, reducing the swelling and erosion of the tablet. In the pH 6.8 condition, the CMC is highly ionized, thus resulting in a faster release.[62,63]

The pH-dependent drug release behavior was observed in series 3 and 4 formulations. The observed faster release in pH 6.8 compared to the water medium might be related to the ionization of CMC in different pH conditions that resulted in different release profiles. The carboxylic acid groups in the CMC become more ionized at higher pH, which induces the

polymer network expansion by electrostatic repulsion. This increases swelling behavior in the matrix system, leading to diffusion. In contrast, CMC becomes less ionized in water due to fewer hydroxide ions. Therefore, there is less expansion in the polymer network by electrostatic repulsion, leading to slow erosion, thus resulting in slow diffusion.[62,64]

The surface area to volume ratio is considered an essential factor, as it influences the drug release of tablets with different surface areas. Therefore, the next goal was to understand the release behavior of ER formulation drug-loaded tablet sizes 4.5, 7.5, 15, and 22.5, as shown Fig. 6b. The study was conducted in pH 6.8 buffer medium for 0–12 h. Sizes 4.5 and 7.5 showed similar releasing profiles, releasing the drug at 7 and 8 h, respectively. Sizes 15 and 22.5 showed similar profiles by releasing the drug within 10 h; no significant differences were found.

The smaller sizes of 4.5 and 7.5 are likely to have a higher surface area/volume ratio than the larger sizes of 15 and 22.5. The pore size of the 3D printed tablet structures can also potentially affect the release rate by penetrating through the matrix system and accelerating the drug release.[65] Despite being 3D printed with a 100% infill rate of grid patterns, noticeable porosity was observed in the different-sized tablets after drying. This porosity influences the release profile by affecting factors such as fluid penetration, interactions with a swelling and erosion process, and drug distribution within the tablet matrix.[66–69] The smaller tablets, 4.5 and 7.5, might have a similar internal structure and compactions. However, the ratio of drug to polymer may vary when comparing smaller tablets with larger tablets. These differences can lead to quick swelling behavior, resulting in faster drug release. Tablets 15 and 22.5 are larger in size and mass than the smaller ones and could affect the overall release performance. Moreover, the tablet layers with complex internal structures of the larger tablets might influence the diffusion path to be longer than in smaller tablets, which allows the drug molecules to travel a longer distance within the tablet matrix, preventing them from being released quickly and leading to a slow release rate.[70]

Drug release kinetics. Several mathematical models have been used to describe the drug dissolution rate in the matrix tablet and understand its kinetic release mechanism. This study investigated six different kinetic models to explain the release mechanism and kinetic orders of four other series and tablets of various sizes. The obtained coefficient of different kinetic models R^2 and the n (release exponent) values calculated from the Korsmeyer-Peppas model that characterizes the release mechanism of the drug are plotted in Table 3, and the different kinetic fits are shown in Fig. S7.† Series 1 best fits the Weibull model (R^2 = 0.9962). Series 2 best fits Weibull and Korsmeyer-Peppas (R^2 = 0.9967 and 0.9993, respectively). The obtained n values indicate a non-Fickian transport mechanism, meaning multiple processes control the drug release, such as diffusion and erosion. Series 3 demonstrated the best fit for the Korsmeyer-Peppas and Weibull models, with R^2 values of 0.9933 and 0.9970, respectively. Series 4 showed the best fit for Korsmeyer-Peppas with an R^2 of 0.9903. Both series indicate Fickian diffusion, with an n value of less than 0.5, meaning the diffusion mechanism primarily controls drug release.

Sizes 4.5 and 7.5 showed the closest best fits for the first-order, Korsmeyer-Peppas, and Weibull methods. The n value indicates non-Fickian transport. Sizes 15 and 22.5 show a close fit to Korsmeyer-Peppas and Weibull by following non-Fickian transport. In conclusion, most formulations exhibit complex release through diffusion and erosion mechanisms. However, all the different formulations showed poor correlation with zero-order release, probably due to the influence of the initial burst release of the drug from the tablet surface.

Savaser *et al.* reported that the sustained release matrix system formulations containing MCP explored in their study indicated non-Fickian diffusion (n value ranges between 0.415 and 0.676). Hence, the drug release is followed by more than one process.[5] Abdel-Rahman *et al.* prepared sustained-release MCP tablets with n values between 0.583 and 0.758, indicating a combination of chain relaxation and diffusion drug release mechanisms in the prepared MCP tablets.[71] Both research studies have considered the corresponding n values to indicate the tablet matrix release mechanism, which aligns with our study's findings (Table 3).

In conclusion, the amount of polymer influences the drug release. Therefore, the polymer concentration can be increased for a more prolonged duration of drug release. In this study, the prepared formulation showed drug release over an extended period of 12 h in pH 6.8, and the release mechanism was controlled by diffusion and erosion of the tablet matrix.

Stability study. The drug content and ATR-FTIR studies were carried out on the stored size 15 dual-release tablets for up to 2 months. Due to the low drug concentration, excipients domi-

Table 3 Kinetic release models of metoclopramide containing dual-release tablets and n values obtained from the Korsmeyer–Peppas model

Names of formulations	Zero-order R^2	First-order R^2	Higuchi R^2	Hixon Crowell R^2	Korsmeyer-Peppas R^2	Weibull R^2	n values
Series 1	0.6277	0.9826	0.8835	0.9826	0.8925	0.9962	0.670
Series 2	0.9004	0.9862	0.9925	0.9719	0.9993	0.9967	0.580
Series 3	0.7043	0.9184	0.9821	0.8704	0.9933	0.9970	0.418
Series 4	0.7453	0.9022	0.9842	0.8689	0.9903	0.9782	0.435
Size 4.5	0.9121	0.9947	0.9825	0.9832	0.9954	0.9979	0.612
Size 7.5	0.9341	0.9932	0.9737	0.9847	0.9949	0.9958	0.651
Size 15	0.9012	0.9907	0.9918	0.9788	0.9987	0.9966	0.581
Size 22.5	0.9168	0.9939	0.9864	0.9850	0.9988	0.9963	0.602

nated the observed peaks of MCP in the IR layer, but the peaks were identified in the ER layer of the tablet. Nevertheless, the presence of the drug in the tablet was confirmed by the drug content study. The measured drug content was compared with the day 1 analysis, which was found to be 17.03 ± 0.81, 18.75 ± 1.67, and 17.74 ± 1.06 mg for day 1, months 1, and 2, respectively. There are no statistically significant changes in the drug content over time. This confirms the stability of MCP in the tablet upon storage.

Conclusions

In this study, we have successfully employed SSE 3D printing technology to manufacture tailored dual-release tablets containing metoclopramide. Four different sizes of tablets were designed for both immediate-release formulations with a quick burst and extended-release formulations for prolonged therapeutic effects. The tailored doses showed strong correlations between tablet area and the obtained drug amount in fabrication, confirming the suitability of SSE 3D printing for producing tailored doses. SEM revealed distinct morphological differences between immediate and extended-release formulations. The 3D printed tablets exhibited sufficient mechanical strength to withstand post-manufacturing processes. The formulations contained primary matrix formers and release-modifying polymers, such as HPC, CMC, and EC, to investigate how they influenced the dissolution release profile in different pH environments. Various kinetic models were applied to evaluate the release mechanisms of the matrix tablets, which were controlled by a combination of diffusion and erosion processes.

In conclusion, this study presents a formulation approach with a promising on-demand manufacturing technique for achieving tailored dual-release tablets close to the point-of-care. The efficiency of printing time to fabricate tablets suggests the suitability for rapid prototyping and enhances the feasibility of formulation development in pharmaceutical research. Our finding opens up new opportunities for addressing treatments that require frequent administration, potentially leading to improved patient compliance with safe treatment, especially in veterinary medicine.

Author contributions

Conceptualization and methodology: R. Mathiyalagan, E. Monaco, and X. Wang; formal analysis: R. Mathiyalagan, R. Altunay, J. Suuronen; data curation, R. Mathiyalagan, M. Westerlund; investigation: R. Mathiyalagan, M. Westerlund; visualization and validation: R. Mathiyalagan, A. Mahran, M. Palo, J. O. Nyman, and X. Wang; supervision: E. Immonen, J. M. Rosenholm, E. Monaco, and X. Wang; resources, funding acquisition and project administration: E. Immonen, J. M. Rosenholm, X. Wang; writing – original – draft: R. Mathiyalagan; writing – review & editing: A. Mahran, R. Altunay, J. Suuronen, M. Palo, J. O. Nyman, E. Immonen, E. Monaco, J. M. Rosenholm, and X. Wang.

Data availability

The dataset supporting this study is openly available in a public repository at https://zenodo.org, accessible through the following link: **https://doi.org/10.5281/zenodo.14870320**.

Conflicts of interest

There are no conflicts of interest declared.

Acknowledgements

References

1 Middlehope Veterinary Hospital. Vomiting in Dogs and Cats: Causes, Treatment, and Prevention [Internet]. Available from: **https://www.middlehopevet.com/blog/2021/june/vomiting-in-dogs-and-cats-causes-treatment-and-p/**.

2 A. L. Moyer, T. S. McKee, P. J. Bergman and A. Vinayak, Low incidence of postoperative nausea, vomiting, regurgitation, and aspiration pneumonia in geriatric dogs receiving maropitant, famotidine, and fentanyl as part of an anesthesia protocol, *J. Am. Vet. Med. Assoc.*, 2022, **260**(S1), S46–S51.

3 A. M. Holmes, J. A. Rudd, F. D. Tattersall, Q. Aziz and P. L. R. Andrews, Opportunities for the replacement of animals in the study of nausea and vomiting, *Br. J. Pharmacol.*, 2009, **157**(6), 865–880.

4 A. G. Stosik, H. E. Junginger, S. Kopp, K. K. Midha, V. P. Shah, S. Stavchansky, J. B. Dressman and D. M. Barends, Biowaiver Monographs for Immediate Release Solid Oral Dosage Forms: Metoclopramide Hydrochloride, *J. Pharm. Sci.*, 2012, **97**, 3700–3708.

5 A. Savaşer, Ç. Taş, Z. Bayrak, C. K. Özkan and Y. Özkan, Effect of different polymers and their combinations on the release of metoclopramide HCl from sustained-release hydrophilic matrix tablets, *Pharm. Dev. Technol.*, 2013, **18**(5), 1122–1130.

6 R. Bernardo-Escudero, R. Alonso-Campero, M. T. De Jesú s Francisco-Doce, M. Cortés-Fuentes, M. Villa-Vargas and J. Ángeles-Uribe, Comparison of the pharmacokinetics of a new 30 mg modified-release tablet formulation of metoclopramide for once-a-day administration versus 10 mg immediate-release tablets: A single and multiple-dose, randomized, open-label, parallel study in healthy mal, *Eur. J. Drug Metab. Pharmacokinet.*, 2012, **37**(4), 279–288.

7 C. Livermore, H. White, L. Bailey, I. Osborne, E. Oloyede, O. Dzahini, *et al.*, A retrospective case notes review of the effectiveness and tolerability of metoclopramide in the treatment of clozapine-induced hypersalivation (CIH), *BMC Psychiatry*, 2022, **22**(1), 1–6, DOI: 10.1186/s12888-022-03940-0.

8 R. Narayanasamy and R. Shabaraya, Preparatıon and Evaluatıon of a Sustaıned Release Formulatıon of Metoclopramıde Hydrochlorıde Hpmc Tablets, *Marmara Pharm. J.*, 2017, **21**(3), 717–717.

9 MSD, Veterinary Manual, Prokinetic Drugs, https://www.msdvetmanual.com/multimedia/table/prokinetic-drugs (accessed November 2024).

10 European Medicines Agency, Assessment Report: Metoclopramide-Only Containing Medicinal Products, EMA/753989/2013, 2013.

11 European Medicines Agency, European Medicines Agency recommends changes to the use of metoclopramide, EMA/13239/2014 Corr. 1, 2013.

12 R. Gollakner, Metoclopramide [Internet]. vca animal hospitals. Available from: https://vcahospitals.com/know-your-pet/metoclopramide.

13 D. D. Primovic, Metoclopramide HCl (Reglan®) for Dogs and Cats [Internet]. Pet place. Available from: https://www.petplace.com/article/drug-library/drug-library/library/metoclopramide-hcl-reglan-for-dogs-and-cats.

14 G. Davidson, Veterinary compounding: Regulation, challenges, and resources, *Pharmaceutics*, 2017, **9**(1), 5.

15 F. Laffleur and V. Keckeis, Advances in drug delivery systems: Work in progress still needed?, *Int. J. Pharm.:X*, 2020, **2**, 1–17.

16 D. Liu, F. Yang, F. Xiong and N. Gu, The smart drug delivery system and its clinical potential, *Theranostics*, 2016, **6**(9), 1306–1323.

17 R. R. Bhagwat and I. S. Vaidhya, Novel Drug Dilvery System: An Overview, *Int. J. Pharma Sci. Res.*, 2013, **4**(3), 970–982.

18 M. Cui, Y. Yang, D. Jia, P. Li, Q. Li, F. Chen, *et al.*, Effect of novel internal structures on printability and drug release behavior of 3D printed tablets, *J. Drug Delivery Sci. Technol.*, 2019, **49**, 14–23, DOI: 10.1016/j.jddst.2018.10.037.

19 S. Ayyoubi, J. R. Cerda, R. Fernández-García, P. Knief, A. Lalatsa, A. M. Healy, *et al.*, 3D printed spherical mini-tablets: Geometry versus composition effects in controlling dissolution from personalised solid dosage forms, *Int. J. Pharm.*, 2021, **597**, 1–32.

20 T. Blicharski, K. Swiader, A. Serefko, S. Kulczycka-Mamona, M. Kolodziejczyk and A. Szopa, Challenges in technology of bilayer and multi-layer tablets: A mini-review, *Curr. Issues Pharm. Med. Sci.*, 2019, **32**(4), 229–235.

21 M. Akhtar, M. Jamshaid, M. Zaman and A. Z. Mirza, Bilayer tablets: A developing novel drug delivery system, *J. Drug Delivery Sci. Technol.*, 2020, **60**, 102079, DOI: 10.1016/j.jddst.2020.102079.

22 A. Singh, S. Das, S. Gupta and S. Ghosh, The Challenges of Producing Bilayer Tablet: A Review, *J. Drug Delivery Ther.*, 2021, **11**(4-S), 171–175.

23 H. S. Yang and D. W. Kim, Fabrication of Gastro-Floating Famotidine Tablets: Hydroxypropyl Methylcellulose-Based Semisolid Extrusion 3D Printing, *Pharmaceutics*, 2023, **15**(2), 316.

24 X. Y. Teoh, B. Zhang, P. Belton, S. Y. Chan and S. Qi, The Effects of Solid Particle Containing Inks on the Printing Quality of Porous Pharmaceutical Structures Fabricated by 3D Semi-Solid Extrusion Printing, *Pharm. Res.*, 2022, **39**(6), 1267–1279, DOI: 10.1007/s11095-022-03299-7.

25 S. A. Khaled, M. R. Alexander, D. J. Irvine, R. D. Wildman, M. J. Wallace, S. Sharpe, *et al.*, Extrusion 3D Printing of Paracetamol Tablets from a Single Formulation with Tunable Release Profiles Through Control of Tablet Geometry, *AAPS PharmSciTech*, 2018, **19**(8), 3403–3413.

26 I. Bácskay, Z. Ujhelyi, P. Fehér and P. Arany, The Evolution of the 3D–Printed Drug Delivery Systems, *Rev. Pharm.*, 2022, **14**(7), 1312.

27 N. Kottala, A. Abebe, O. Sprockel, J. Bergum, F. Nikfar and A. M. Cuitiño, Evaluation of the performance characteristics of bilayer tablets: Part I. Impact of material properties and process parameters on the strength of bilayer tablets, *AAPS PharmSciTech*, 2012, **13**(4), 1236–1242.

28 P. A. Haran, A. S. Pratapwar, M. M. Thakre and A. R. Haran, Bilayer tablet: an dual release drug delivery system, *Journal of Emerging Technologies and Innovative Research (JETIR)*, 2024, **11**(1), 161–169.

29 H. G. Lee, Y. S. Park, J. H. Jeong, K. Y. Bin, D. H. Shin, J. Y. Kim, *et al.*, Physicochemical properties and drug-release mechanisms of dual-release bilayer tablet containing mirabegron and fesoterodine fumarate, *Drug Des., Dev. Ther.*, 2019, **13**, 2459–2474.

30 J. Goole and K. Amighi, 3D printing in pharmaceutics: A new tool for designing customized drug delivery systems, *Int. J. Pharm.*, 2016, **499**(1–2), 376–394.

31 B. Zhang, X. Y. Teoh, J. Yan, A. Gleadall, P. Belton, R. Bibb, *et al.*, Development of combi-pills using the coupling of semi-solid syringe extrusion 3D printing with fused deposition modelling, *Int. J. Pharm.*, 2022, **625**, 122140, DOI: 10.1016/j.ijpharm.2022.122140.

32 A. G. Crişan, A. Porfire, S. Iurian, L. M. Rus, R. Lucăcel Ciceo, A. Turza, I. Tomuţă, *et al.*, Development of a Bilayer Tablet by Fused Deposition Modeling as a Sustained-Release Drug Delivery System, *Pharmaceuticals*, 2023, **16**(9), 1321.

33 N. Genina, J. P. Boetker, S. Colombo, N. Harmankaya, J. Rantanen and A. Bohr, Anti-tuberculosis drug combination for controlled oral delivery using 3D printed compartmental dosage forms: From drug product design to in vivo testing, *J. Controlled Release*, 2017, **268**, 40–48, DOI: 10.1016/j.jconrel.2017.10.003.

34 A. Ghanizadeh Tabriz, U. Nandi, A. P. Hurt, H. W. Hui, S. Karki, Y. Gong, S. Kumar, D. Douroumis, *et al.*, 3D printed bilayer tablet with dual controlled drug release for tuberculosis treatment, *Int. J. Pharm.*, 2021, **593**, 120147, DOI: 10.1016/j.ijpharm.2020.120147.

35 S. A. Khaled, J. C. Burley, M. R. Alexander and C. J. Roberts, Desktop 3D printing of controlled release pharmaceutical bilayer tablets, *Int. J. Pharm.*, 2014, **461**(1–2), 105–111, DOI: 10.1016/j.ijpharm.2013.11.021.

36 D. Fang, Q. Guan, X. Wang and H. Pan, Exploration and preparation of ofloxacin biphasic tablets via semi-solid extrusion technology, *J. Drug Delivery Sci. Technol.*, 2024, **96**, 105737, DOI: 10.1016/j.jddst.2024.105737.

37 O. A. Adeleke, Premium ethylcellulose polymer based architectures at work in drug delivery, *Int. J. Pharm.:X*, 2019, **1**, 100023, DOI: 10.1016/j.ijpx.2019.100023.

38 R. Mathiyalagan, E. Sjöholm, S. Manandhar, S. Lakio, J. M. Rosenholm, M. Kaasalainen, X. Wang, N. Sandler, *et al.*, Personalizing oral delivery of nanoformed piroxicam by semi-solid extrusion 3D printing, *Eur. J. Pharm. Sci.*, 2023, **188**, 106497.

39 A. Mahran, E. Özliseli, Q. Wang, I. Özliseli, R. Bhadane, C. Xu, *et al.*, Semi–solid 3D printing of mesoporous silica nanoparticle–incorporated xeno–free nanomaterial hydrogels for protein delivery, *Nano Sel.*, 2023, **4**(11–12), 598–614.

40 D. Liepsch, A Basic Introduction to Rheology Shear Flow, *J. Biomech.*, 2016, **35**(4), 415–435. Available from: https://cdn.technologynetworks.com/TN/Resources/PDF/WP160620BasicIntroRheology.pdf.

41 H. Jun, H. J. Lee, B. S. Shin and C. W. Park, Preparation and in vivo characterization of dual release tablet containing sarpogrelate hydrochloride, *J. Pharm. Invest.*, 2018, **48**(3), 363–372.

42 X. R. Adhansia, Methylphenidate Hydrochloride, *FDA*, 2016, 1–23.

43 European Pharmacopoeia, Friability of Uncoated Tablets in European Pharmacopoeia, 2019, 10:0, 336–337.

44 B. Siva Sai Kiran, P. Sambasiva Rao, G. Raveendra Babu and M. VenkatKumari, Bilayer tablets - A review, *Int. J. Pharm., Chem. Biol. Sci.*, 2015, **5**(3), 510–516.

45 W. Ahsan, S. Alam, S. Javed, H. Alhazmi, M. Albratty, A. Najmi, *et al.*, Mathematical Modeling of Drug Release Kinetics of Different Brands of Rosuvastatin Calcium IR Tablets Marketed in Saudi Arabia, *Dissolution Technol.*, 2022, 1–12.

46 W. Zhu, J. Long and M. Shi, Release Kinetics Model Fitting of Drugs with Different Structures from Viscose Fabric, *Materials*, 2023, **16**(8), 3282.

47 C. Corsaro, G. Neri, A. M. Mezzasalma and E. Fazio, Weibull modeling of controlled drug release from Ag-PMA nanosystems, *Polymers*, 2021, **13**(17), 2897.

48 E. Sjöholm, R. Mathiyalagan, D. R. Prakash, L. Lindfors, Q. Wang, X. Wang, *et al.*, 3D-Printed Veterinary Dosage Forms—a Comparative Study of Three Semi-Solid Extrusion 3D Printers, *Pharmaceutics*, 2020, **12**(12), 1–26.

49 J. Ahmad, A. Garg, G. Mustafa, A. A. Mohammed and M. Z. Ahmad, 3D Printing Technology as a Promising Tool to Design Nanomedicine-Based Solid Dosage Forms: Contemporary Research and Future Scope, *Pharmaceutics*, 2023, **15**(5), 1448.

50 R. V. Barrulas and M. C. Corvo, Rheology in Product Development: An Insight into 3D Printing of Hydrogels and Aerogels, *Gels*, 2023, **9**(12), 986.

51 M. S. Latif, A. K. Azad, A. Nawaz, S. A. Rashid, M. H. Rahman, S. Y. Al Omar, S. G. Bungau, L. Aleya and M. M. Abdel Daim, Ethyl cellulose and hydroxypropyl methyl cellulose blended methotrexate-loaded transdermal patches: In vitro and ex vivo, *Polymers*, 2021, **13**(20), 3455.

52 M. V. Ghica, M. Hîrjău, D. Lupuleasa and C. E. Dinu-Pîrvu, Flow and Thixotropic Parameters for Rheological Characterization of Hydrogels, *Molecules*, 2016, **21**(6), 786.

53 Y. Chen, S. Wang, S. Wang, C. Liu, C. Su, M. Hageman, *et al.*, Initial Drug Dissolution from Amorphous Solid Dispersions Controlled by Polymer Dissolution and Drug-Polymer Interaction, *Pharm. Res.*, 2016, **33**(10), 2445–2458, DOI: 10.1007/s11095-016-1969-2.

54 K. Olechno, A. Basa and K. Winnicka, "Success Depends on Your Backbone"—About the Use of Polymers as Essential Materials Forming Orodispersible Films, *Materials*, 2021, **14**(17), 1–27.

55 Y. Li, H. Pang, Z. Guo, L. Lin, Y. Dong, G. Li, *et al.*, Interactions between drugs and polymers influencing hot melt extrusion, *J. Pharm. Pharmacol.*, 2014, **66**(2), 148–166.

56 L. Leon, A. Herbert and J. L. K. Lieberman, The Theory and Practice of Industrial Pharmacy, in *Journal of Pharmaceutical Sciences*, Philadelpia, United stataes, 3rd edn, 1986.

57 D. Karalia, A. Siamidi, V. Karalis and M. Vlachou, 3d–printed oral dosage forms: Mechanical properties, computational approaches and applications, *Pharmaceutics*, 2021, **13**(9), 1401.

58 E. Sjöholm, R. Mathiyalagan, X. Wang and N. Sandler, Compounding Tailored Veterinary Chewable Tablets Close to the Point-of-Care by Means of 3D Printing, *Pharmaceutics*, 2022, **14**(7), 1339.

59 M. S. Reza, M. A. Quadir and S. S. Haider, Comparative evaluation of plastic, hydrophobic and hydrophilic polymers as matrices for controlled-release drug delivery, *J. Pharm. Pharm. Sci.*, 2003, **6**(2), 282–291.

60 P. Pakalapati, Effect of Polymer Concentration on Drug Release in the Formulation of Controlled Release Tablets of Glipizide Using Novel Natural Polymers, *J. Pharm. Sci. Res.*, 2021, **13**(3), 162–169.

61 B. V. K. J. Schmidt, Hydrophilic polymers, *Polymers*, 2019, **11**(4), 1–5.

62 S. Jung, *Hydrogels with Highly Improved Mechanical Strength for Controlled Drug Delivery Systems*, 2021.

63 K. Wasilewska and K. Winnicka, Ethylcellulose-a pharmaceutical excipient with multidirectional application in drug dosage forms development, *Materials*, 2019, **12**(20), 3386.

64 Y. Bao, J. Ma and N. Li, Synthesis and swelling behaviors of sodium carboxymethyl cellulose-g-poly(AA-co-AM-co-AMPS)/MMT superabsorbent hydrogel, *Carbohydr. Polym.*, 2011, **84**(1), 76–82.

65 R. D. Juch and T. C. S. Rufli, Pastes: What Do They Contain? How Do They Work?, *Dermatology*, 1994, **4**(189), 373–377.

66 F. Molavi, H. Hamishehkar and A. Nokhodchi, Impact of tablet shape on drug dissolution rate through immediate released tablets, *Adv. Pharm. Bull.*, 2020, **10**(4), 656–661, DOI: **10.34172/apb.2020.079**.

67 Y. J. Kim, Y. R. Choi, J. H. Kang, Y. S. Park, D. W. Kim and C. W. Park, Geometry-Driven Fabrication of Mini-Tablets via 3D Printing: Correlating Release Kinetics with Polyhedral Shapes, *Pharmaceutics*, 2024, **16**(6), 1–17.

68 H. Windolf, R. Chamberlain and J. Quodbach, Predicting drug release from 3D printed oral medicines based on the surface area to volume ratio of tablet geometry, *Pharmaceutics*, 2021, **13**(9), 1453.

69 B. Zhang, J. Nasereddin, T. McDonagh, D. von Zeppelin, A. Gleadall, F. Alqahtani, *et al.*, Effects of porosity on drug release kinetics of swellable and erodible porous pharmaceutical solid dosage forms fabricated by hot melt droplet deposition 3D printing, *Int. J. Pharm.*, 2021, **604**, 120626, DOI: **10.1016/j.ijpharm.2021.120626**.

70 P. Narayana Raju, K. Prakash, T. Rama Rao, B. C. S. Reddy, V. Sreenivasulu and M. Lakshmi Narasu, Effect of Tablet Surface Area and Surface Area/Volume on Drug Release from Lamivudine Extended Release Matrix Tablets, *Int. J. Pharm. Sci. Nanotechnol.*, 2010, **3**(1), 872–876.

71 S. I. Abdel-Rahman, G. M. Mahrous and M. El-Badry, Preparation and comparative evaluation of sustained release metoclopramide hydrochloride matrix tablets, *Saudi Pharm. J.*, 2009, **17**(4), 283–288, DOI: **10.1016/j.jsps.2009.10.004**.